

Special
Collection

Electrochemical Immobilisation of Glucose Oxidase for the Controlled Production of H₂O₂ in a Biocatalytic Flow Reactor

Simin Arshi,^[a] Xinxin Xiao,^[b] Serguei Belochapkin,^[a] and Edmond Magner^{*[a]}*Dedicated to Professor Plamen Atanassov on the occasion of his 60th birthday*

Electrochemical methods can be used to selectively modify the surfaces of electrodes, enabling the immobilisation of enzymes on defined areas on the surfaces of electrodes. Such selective immobilisation methods can be used to pattern catalysts on surfaces in a controlled manner. Using this approach, the selective patterning of the enzyme glucose oxidase on the electrodes was used to develop a flow reactor for the controlled delivery of the oxidant H₂O₂. GOx was immobilised on a glassy carbon electrode using polypyrrole, silica films, and diazonium linkers. The rate of production of H₂O₂ and the stability of the response was dependent on the immobilisation method. GOx

encapsulated in polypyrrole was selected as the optimal method of immobilisation, with a rate of production of $91 \pm 11 \mu\text{M h}^{-1}$ for 4 hours of continuous operation. The enzyme was subsequently immobilised on carbon rod electrodes (surface area of 5.76 cm²) using a polypyrrole/Nafion[®] film and incorporated into a flow reactor. The rate of production of H₂O₂ was $602 \pm 57 \mu\text{M h}^{-1}$, with 100% retention of activity after 7 h of continuous operation, demonstrating that such a system can be used to prepare H₂O₂ at continuous and stable rate for use in downstream oxidation reactions.

Introduction

The immobilisation of enzymes has been used extensively to improve the stability (particularly under harsh conditions), the ability to reuse and the ease of separation of the catalyst from solution.^[1,2] The ability to reuse an enzyme can be particularly advantageous in flow systems.^[3] A wide range of materials have been used for the immobilisation of enzymes, including polymers,^[4] inorganic materials,^[5] sol-gels,^[6] and organic films.^[7] Immobilisation can be classified under five broad categories:^[8] physical adsorption, covalent binding, ionic interactions, cross-linking, and entrapment.


Cross linked enzyme aggregates (CLEA) and cross-linked enzyme crystals (CLEC),^[9] and adsorption processes^[10] have been used extensively for the immobilisation of enzymes. However, the use of CLEA and CLEC in flow systems is limited while CLEA suffer from disadvantages such as poor reproducibility and low mechanical stability. Immobilisation via adsorption results in low stability and leaching of the enzyme.^[9,10]


Electrochemical methods provide a controlled, facile and rapid means of immobilising enzymes on conductive supports.^[11] The properties of enzyme modified films can be controlled by altering the potential of the electrode and/or adjusting the electrodeposition conditions.^[12] Electrochemical reduction of diazonium salts provides a modified electrode surface that is suitable for the covalent attachment of enzymes.^[13] Silica-based materials have been used for the encapsulation of enzymes. Electrodeposition of silica films can be achieved via the electrochemical production of hydroxyl ions that catalyse the condensation of alkoxy silane precursors.^[14–16] Conducting polymers such as polyaniline, polypyrrole and poly(3,4-ethylenedioxythiophene) have been used for the immobilisation of enzymes.^[17,18] In this approach, immobilisation is performed via electropolymerization in a solution containing the enzyme and the appropriate monomer.^[19] Polypyrrole has been very extensively used for the immobilisation of enzymes to prepare biosensors.^[20–22] Pyrrole is easily oxidized, water-soluble, and polypyrrole possesses good conductivity and stability and adheres tightly to the surfaces of electrodes.^[23,24]


Electrochemical methods of enzyme immobilisation have primarily focussed on applications such as biosensors^[25,26] and biofuel cells.^[27] This approach can also be used for the immobilisation of enzymes for applications in, e.g. biocatalysis, where the electrode is used as a support rather than as an electrode per se. For example, lipase was encapsulated in an electrochemically generated silica film in nanoporous gold supports. In a flow reactor, the hydrolysis of 4-nitrophenyl butyrate (4-NPB) was achieved with 100% conversion

[a] S. Arshi, Dr. S. Belochapkin, Prof. E. Magner
Department of Chemical Sciences, Bernal Institute
University of Limerick
V94 T9PX Limerick, Ireland
E-mail: edmond.magner@ul.ie

[b] Dr. X. Xiao
Department of Chemistry
Technical University of Denmark
Kongens Lyngby 2800, Denmark

 Supporting information for this article is available on the WWW under <https://doi.org/10.1002/celec.202200319>

 An invited contribution to the Plamen Atanassov Festschrift

 © 2022 The Authors. ChemElectroChem published by Wiley-VCH GmbH. This is an open access article under the terms of the Creative Commons Attribution Non-Commercial License, which permits use, distribution and reproduction in any medium, provided the original work is properly cited and is not used for commercial purposes.

efficiency.^[11] Electrochemically prepared self-assembled monolayers were used to sequentially and independently immobilise alcohol dehydrogenase (ADH), formaldehyde dehydrogenase (FLDH), and formate dehydrogenase (FoDH) on three separate electrodes.^[28]

Hydrogen peroxide (H_2O_2) can be considered as an environmentally friendly oxidant in chemical synthesis.^[29] It provides 47% of its mass as an oxidant, and water and oxygen are the only by-products in the reaction.^[30] In addition to using H_2O_2 in a range of processes, its application in enzymatic synthesis is receiving increased interest.^[29] Hydrogen-peroxide dependent biocatalysts have been used in a range of reactions, such as the selective oxyfunctionalisation of non-activated C–H bonds.^[29] However, H_2O_2 is a strong oxidant, and excess amounts of H_2O_2 can be deleterious to enzymes.^[30,31] Considerable efforts based on photocatalysis,^[32] electrocatalysis^[33] and enzymatic^[34] methods have been made to prepare H_2O_2 in situ at constant low concentrations to mitigate this issue.^[29] Electrochemical methods entail the oxidation of water at the anode or reduction of oxygen at the cathode.^[35] A photoelectrochemical (PEC) system based on the oxidation of water at an $\text{FeOOH}/\text{BiVO}_4$ photoanode resulted in a rate of production of H_2O_2 of $2.8 \text{ mMh}^{-1} \text{ cm}^{-2}$ and was subsequently used for the peroxylase catalysed stereoselective hydroxylation of ethylbenzene to (R)-1-phenylethanol.^[33] Another PEC approach was based on the illumination of use of flavin-modified single-walled carbon nanotube electrodes to yield a rate of production of 0.15 mMh^{-1} .^[31] An example of an electrocatalytic approach is the preparation of H_2O_2 on graphite felt electrodes at a rate of 5.27 mMh^{-1} .^[36] Electrochemical methods can generate radicals that are capable of inactivating enzymes. Enzymatic approaches do not suffer from such limitations and are an alternative method for the in situ generation of H_2O_2 . Oxidases such as glucose oxidase,^[37] cholesterol oxidase,^[38] and formate oxidase^[34] have been used for the in situ preparation of H_2O_2 . For example, formate oxidase was used to generate H_2O_2 for halogenation reactions catalyzed by V-dependent haloperoxidase,^[34] while alcohol oxidase (AOx) and formaldehyde dismutase (FDM) were used to prepare H_2O_2 from methanol.^[39]

Glucose oxidase (GOx) is a flavoprotein catalyzing the oxidation of β -D-glucose to D-glucono- δ -lactone, using molecular oxygen as an electron acceptor and generating H_2O_2 as the by-product.^[40] It is available at low cost and is a relatively robust enzyme.^[29] GOx has been used in a number of studies for the in situ generation of H_2O_2 .^[37,41] For example, GOx was immobilised on SBA-15 with an initial rate of formation of H_2O_2 of $0.303 \mu\text{mol min}^{-1}$ and used for the chloroperoxidase (CPO) catalyzed oxidation of indole to 2-oxindole.^[42] CPO is easily inactivated in the presence of H_2O_2 and requires the controlled addition of H_2O_2 at low concentrations.^[43,44] The operational stability of peroxidases can be increased considerably by producing H_2O_2 in situ using glucose oxidase.^[41,42,45] While GOx has been used for the preparation of H_2O_2 , inactivation of the enzyme by H_2O_2 hinders its use.^[46] Effective immobilisation of GOx in a suitable matrix can be effectively used to increase its stability during continuous operation in a flow system. Here,

different approaches based on the use of polymers, direct coupling (based on diazonium coupling), and silica films have been evaluated for the immobilisation of GOx on electrodes to produce H_2O_2 in situ in a stable and controlled manner. Enzymatic production of H_2O_2 is competitive with photoelectrochemical and electrochemical methods. Then, immobilised GOx is incorporated in a flow reactor.

Results and Discussion

Immobilisation of GOx on GCE surface

Four methods of immobilising GOx on the surface of an electrode (Figure 1) were evaluated to ascertain the optimal method of preparing hydrogen peroxide in a controlled manner. A glassy carbon electrode was used initially, screen printed carbon inks and graphite rods with higher surface areas were subsequently evaluated as supports. Nitrophenyl diazonium tetrafluoroborate and 2-carboxy-6-naphthoyl diazonium chloride were used to produce layers containing amino and carboxyl terminal groups, respectively.^[47,48] A nitrophenyl modified electrode surface (Figure 1A) was prepared by scanning the potential for two cycles (Figure 2A). A broad reduction peak occurred at 0.18 V in the first cycle, while in the second cycle a considerable decrease in the cathodic current was observed that can be attributed to the covalent attachment of nitrophenyl groups on to the electrode surface (Figure S1A). The nitrophenyl layer was then reduced to an aminophenyl layer, as evidenced by the broad cathodic peak at -0.9 V (Figure S1B). The concentration of the aminophenyl layer was $1.3 \pm 0.05 \text{ nmol cm}^{-2}$, indicative of a surface coverage of 93%. The cathodic peak disappeared after the second potential scan, indicative of complete reduction of the nitrophenyl layer.^[49] GOx was then immobilised onto the surface by cycling the potential between -1.0 and 1.2 V . GOx is negatively charged at pH 7.0, the use of a relatively high positive potential of up to 1.2 V is likely to promote electrostatic attraction between the electrode surface and the free enzyme.^[50]

In the second approach (Figure 1B), GC electrodes were modified with 6-amino-2-naphthoic acid by cycling the potential between 0.6 and -0.5 V in a solution of 2-carboxy-6-naphthoyl diazonium salt. A $20 \mu\text{L}$ aliquot of a solution of GOx was drop-cast on the electrode surface followed by CMC as a linker. A number of single step immobilisation methods were employed. Encapsulation of GOx in silica was performed via an electrochemically induced sol-gel process (Figure 1D). A cathodic potential of -1.2 V vs. Ag/AgCl was applied to the electrode, triggering the condensation of TEOS through the production of hydroxyl ions, encapsulating the enzyme in the silica-gel.^[11,16] Entrapment of GOx in PPy was performed by a one-step amperometric polymerization process on the application of a potential of 0.85 V vs. Ag/AgCl. PEDOT was also used for GOx immobilisation on GCE, however the monomer material is only moderately stable in water, restricting its use. When GOx was immobilised in PEDOT films, the response of the modified electrodes decreased rapidly with 35% loss of initial activity

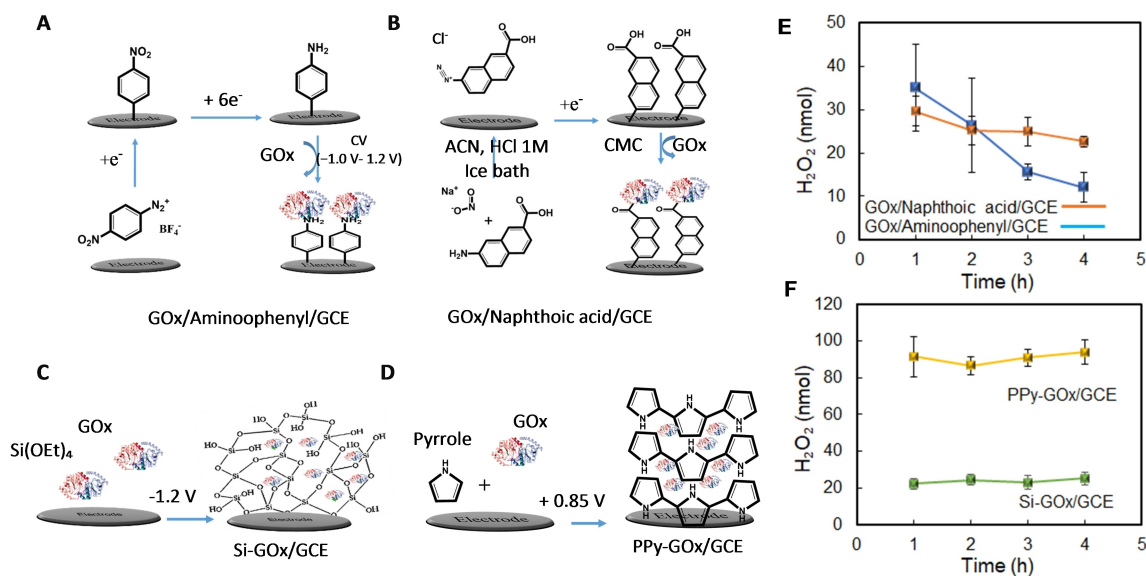


Figure 1. Schematic diagram of the immobilisation of GOx on a glassy carbon electrode (GCE). (A) Coupling of nitrophenyl diazonium tetrafluoroborate to GCE by cycling the potential between 0.4 to -0.3 V at 100 mV s^{-1} (2 cycles), followed by formation of the amine derivative by cycling the potential between 0.7 and -1.2 V at 200 mV s^{-1} (5 cycles) with immobilisation of GOx by cycling the potential between -1.0 and 1.2 V (25 cycles); (B) Coupling of 2-carboxy-6-naphthoic acid diazonium chloride to GCE by cycling the potential between 0.6 – 0.5 V at 200 mV s^{-1} (1 cycle) followed by immobilisation of GOx; (C) Encapsulation of GOx in silica-gel on the application of a potential of -1.2 V (120 s); (D) Encapsulation of GOx via the electropolymerization of pyrrole at 0.85 V (300 s). The time course of the amount of H_2O_2 produced at (E) GOx/naphthoic acid/GCE (—) and GOx/aminophenyl/GCE (—) electrodes. Conditions: 0.5 ml of 30 mM glucose (1 ml stirred solution for GOx/naphthoic acid/GCE; fresh solution for the measurement of each data point); (F) PPy-GOx/GCE (—) (300 s deposition time, 2 mg ml^{-1} GOx), Si-GOx/GCE (—) electrodes. (1 mg ml^{-1} GOx, 1 ml of 30 mM glucose; fresh solution for the measurement of each data point), Condition: 0.1 M pH 7 phosphate buffer, purged with O_2 .

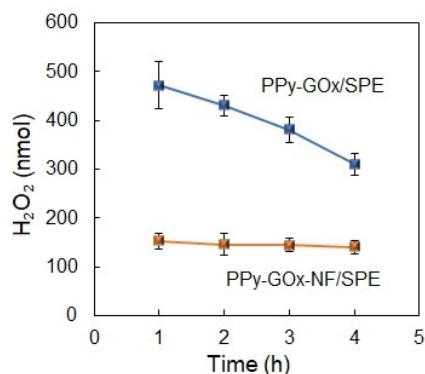


Figure 2. The time course of the production of H_2O_2 at a PPy-GOx/SPE (300 s deposition time, 1 mg ml^{-1} GOx), PPy-GOx-NF/SPE (0.2 M pyrrole, 300 s deposition time, 5 $\mu\text{l ml}^{-1}$ NF, Condition: 0.1 M pH 7 phosphate buffer, 1 ml of 30 mM glucose, purged with O_2).

after the first hour. With such a decrease, the support was not considered for further investigation.

Generation of hydrogen peroxide from immobilised GOx

The rate of production of hydrogen peroxide was investigated by immersing the modified electrodes into solutions of glucose (30 mM) for a period of one hour and replaced with fresh solution each hour for a total of 4 hours. Figure 1E shows the performance of GOx covalently attached to the surface of the electrode by a diazonium linker. On a GOx/aminophenyl

modified electrode 35 ± 10 nmol of H_2O_2 was produced in the first hour, retaining only 35% of initial activity after 4 h. The loss of operational stability is likely due to the detachment of enzyme from the electrode surface. Using a carboxy-6-naphthoic acid modified layer, GOx was immobilised using CMC as a linker. In comparison with the aminophenyl modified layer, the naphthoic acid layer resulted in a more stable response. The production of peroxide was examined under stirred conditions, as the amounts produced in unstirred solution were too low. Under stirring, the modified electrode produced ca. 30 nmol H_2O_2 in the first hour, retaining 76% of initial activity after 4 h of continuous operation. As expected, covalently bound GOx had superior operational stability when compared with that of the physically adsorbed enzyme. Further investigations were performed to increase the operational stability and the activity of the immobilised GOx. The activity of GOx entrapped in silica gel was examined (Figure S2).

A previous study showed that while the enzyme loading increased with deposition time, thicker films presented a diffusion barrier to the substrate, glucose.^[11] A short deposition time (100 s) resulted in a film where 15 ± 2 nmol H_2O_2 was produced in the first hour, increasing to 22 ± 3 nmol for a slightly longer deposition time of 120 s. An additional increase in the electrodeposition time (to 240 s) led to a decrease to 10 nmol, likely arising from impeded rates of diffusion of the substrate into the film. The observed trend is in agreement with previous results.^[51,52] The modified electrodes prepared at each deposition time showed good stability, retaining full activity after 4 hours of continuous operation. The concentration of

GOx was increased to 2 mg mL^{-1} , however precipitation of silica in solution occurred, therefore the concentration of GOx was maintained at 1 mg mL^{-1} . The preparation of PPy/GOx electrodes was optimized in terms of electrodeposition time and the concentration of GOx (Figure S3). Using a deposition solution containing 1.2 mg mL^{-1} GOx and 0.2 M pyrrole (Figure S3A) resulted in the generation of $41 \pm 7 \text{ nmol H}_2\text{O}_2$ in the first hour, with a loss of 24% of activity after 4 hours of continuous operation. The decrease in stability may arise from the short (100 s) electrodeposition time used, resulting in a thin layer of the polymer. In contrast, a deposition time of 300 s resulted in a stable rate of production of H_2O_2 ($40 \pm 4 \text{ nmol h}^{-1}$) over 4 h. An extended electrodeposition time of 500 s resulted in the formation of thicker films with reduced permeability to glucose and a decrease in the rate of production of H_2O_2 to $30 \pm 5 \text{ nmol}$. Deposition times of 100, 300, and 500 s resulted in layers with thickness of 8.9 ± 0.5 , 15 ± 0.7 , and $18 \pm 1.4 \text{ nm}$ on the electrode surface, respectively. Using a deposition time of 300 s (Figure S3B), the amount of H_2O_2 produced increased from 34 ± 1.8 to $91 \pm 11 \text{ nmol}$ on increasing the concentration of GOx from 1 to 2 mg mL^{-1} . Additional increases of the concentration of GOx resulted in negligible increases in the rate of generation of H_2O_2 . A stable rate of production (Figure 5C) of $91 \pm 11 \text{ nmol}$ in 4 h was achieved, therefore, a concentration of 2 mg mL^{-1} GOx was used together with a deposition time of 300 s for further studies (Figure S3C). Overall, the PPy-GOx/GCE system showed good stability and higher rates of production of H_2O_2 (Figure 1F (yellow line)) in comparison to silica (Figure 1F (green line)) and aminophenyl and naphthoic acid modified surfaces (Figure 1E) and was selected as the optimal method. Screen printed carbon electrodes (SPE) are commercially available and can be incorporated in flow reactors. The use of SPE as enzyme supports^[53] was evaluated by encapsulating GOx in a polypyrrole layer electrodeposited on SPE (0.12 cm^2). The rate of production of H_2O_2 was $472 \pm 48 \text{ nmol h}^{-1}$ (Figure 2 (blue line)), 5 times higher than that on GCE (0.07 cm^2) (Figure 1 (yellow line)). The double layer capacitance of SPE was 280 mF cm^{-2} , versus 136 mF cm^{-2} for GCE, indicating that the effective surface area of SPE was two-fold higher than that of GCE.

The increased rate of production of H_2O_2 can be partially ascribed to the increased surface area, the additional increase may arise from a higher loading of enzyme. SEM images of PPy-GOx/SPE showed a relatively high surface roughness (Figure 3). However, the amount of H_2O_2 decreased considerably to ca. 300 nmol after 4 h. From the amperometric data recorded for the electrodeposition of the polymer, significant overoxidation of the polymer occurred during deposition on the SPE surface resulting in a loosely branched polymer network.^[54] PPy overoxidation leads to the production of carboxyl groups on the pyrrole ring, disrupting the conjugation of the PPy chain.^[55] A lower electrodeposition potential can avoid such overoxidation,^[54] however, when a potential of 0.7 V was used, a stable polymer layer was not observed. To improve the chemical and physical stability of PPy-GOx/SPE, Nafion® (NF) was incorporated into the PPy film.^[56]

Figure 3C shows an SEM image of PPy-GOx-NF films deposited using a one-step electrochemical co-polymerization

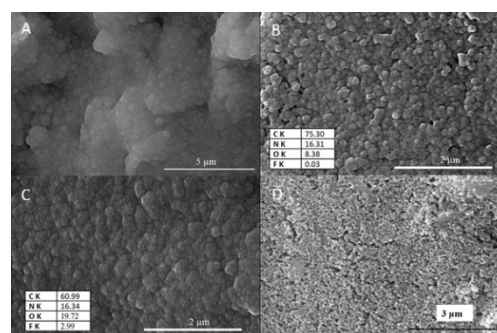


Figure 3. SEM images of (A, B) PPy-GOx/SPE; (C) PPy-GOx-NF/SPE; and (D) bare SPE.

process, with a denser layer observed than that of PPy-GOx/SPE (Figure 3A, B). The electrodeposition time was optimized using 1 mg GOx (Figure S4A). The amount of H_2O_2 produced decreased when the electrodeposition time was increased from 50 to 500 s, likely from the diffusion barrier arising from the increased layer thickness. The electrodeposition time considerably influenced the catalytic activity of the modified electrodes. The stability increased with increasing electrodeposition time from 50 to 300 s, with the highest stability being achieved at 300 s. PPy-GOx-NF/SPE retained 90% of the initial response after 4 hours continuous operation (Figure S4A) with a rate of production of $128 \pm 6 \text{ nmol h}^{-1}$. Therefore, a deposition time of 300 s was selected as the optimized time for the construction of PPy-GOx-NF/SPE. The effect of increasing Nafion® concentration on the stability of modified electrodes was investigated (Figure S4B). The amount of H_2O_2 decreased when the concentration of Nafion® was increased from 2 to $20 \mu\text{L mL}^{-1}$, a decrease that may arise from the increased acidity associated with Nafion® itself or from an increase in the thickness of the polymer layer that limits mass transport.^[57] A concentration of $5 \mu\text{L mL}^{-1}$ Nafion® was selected as the optimal concentration. The effect of GOx concentration was optimised using a deposition time of 300 s, $5 \mu\text{L mL}^{-1}$ Nafion® and 0.2 M pyrrole (Figure S4C). Increasing the concentration of GOx decreased the stability of PPy-GOx-NF/SPE, an effect that may be attributed to reduced rates of polymer formation at higher GOx concentrations that result in lower levels of encapsulation of GOx. The reduced rate of formation of polymer is in good agreement with previous studies,^[58,59] and 1 mg GOx was used as the optimized enzyme concentration. From the results displayed in figure 2, the use of Nafion® increased the stability of PPy-GOx/SPE with retention of 90% of activity versus 63% in the absence of Nafion. The rate of production of H_2O_2 of $1 \text{ Mm h}^{-1} \text{ cm}^2$ achieved on PPy-GOx-NF/SPE with 90% stability retained after 4 hours is comparable with the value reported using graphite felt electrodes ($1.3 \text{ mM h}^{-1} \text{ cm}^{-2}$ in $0.05 \text{ M Na}_2\text{SO}_4$, pH of 3.0) with retention of activity for 2 hours^[36] and lower than that reported for a FeOOH/BiVO₄ photoanode ($2.8 \text{ mM h}^{-1} \text{ cm}^{-2}$, buffer, pH, stability not reported).^[33] The rate is higher than that reported for a flavin-SWNT-based photoelectrochemical platform using light illumination ($0.15 \text{ mM h}^{-1} \text{ cm}^{-2}$, stability not reported).^[31] The optimal method for GOx immobilisation on SPE was used to

immobilise GOx on a graphite rod electrode (GRE, surface area of 5.76 cm²) that was then incorporated into a customised flow cell (Figure 4). The rate of production of H₂O₂ was 602 ± 57 μMh⁻¹, with no loss in activity after 7 hours of continuous operation. In a flow cell, such a high concentration will not be present as the H₂O₂ produced will be removed by the flow. This result demonstrates the stability of GOx in the presence of H₂O₂ at concentrations up to 0.6 mM. The enzyme loading was 1.28 ± 0.2 nmol cm⁻² on the surface of graphite rod. The specific activity of the free enzyme was 133 μmol/min/mg, the activity of the immobilised GOx was significantly lower at 0.03 μmol/min/mg, a decrease that is likely due to diffusional limitations associated with the presence of the polymer.

The PPy-GOx-NF film adhered strongly to the graphite rods and could not be removed easily, even with the use of adhesive tape. After 7 h of continuous operation, the catalytic activity of modified GREs was investigated over a period of 28 days. A stable rate of production of over 1000 nmol h⁻¹ was observed for at least 7 days, with retention of 75% of initial activity after 28 days (Figure 4B). This combination of high mechanical and enzymatic stability clearly demonstrates that these modified electrodes are suitable for long term use in flow reactors.

A flow reactor was designed and constructed (Figure 5) to accommodate the modified graphite rods. The reactor consists

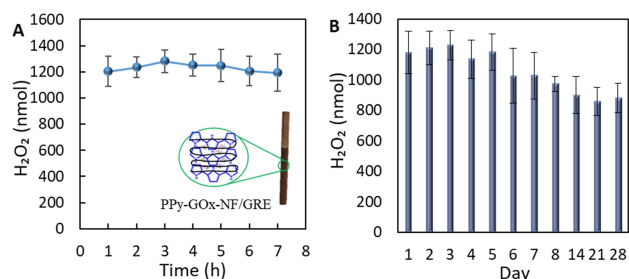


Figure 4. (A) The time course of the production of H₂O₂ at a PPy-GOx-NF/GRE; Inset shows the schematic illustration of PPy-GOx-NF/GRE. (B) The operational stability of GOx-NF/GRE. Condition: 1 mg ml⁻¹ GOx, 0.2 M pyrrole, 300s deposition time, 5 μl ml⁻¹ in 0.1 M pH 7 phosphate buffer, 2 ml of 30 mM glucose, purged with O₂.

of two caps and a cylinder. A PPy-GOx-NF/GRE with a surface area of 4.94 cm² was inserted into the cylinder and the caps placed on both sides of the cylinder. The residence time of the reactor was 6 minutes at a flow rate of 0.02 ml min⁻¹ and a reactor volume of 0.12 cm³. The rate of production of H₂O₂ was monitored for 6 hours of continuous operation, with a rate of production of 41.6 ± 1.8 μMh⁻¹ of H₂O₂ (Figure 5H). In order to investigate the operational stability of the modified electrode in the flow reactor, the activity of GOx on the electrode surface was measured before and after 6 hours of continuous operation in the reactor. When the modified electrodes were immersed in a solution of glucose (30 mM) for 15 minutes, 72% of the initial activity was retained. On increasing the flow rate from 0.02 to 0.06 ml min⁻¹, the activity decreased considerably to less than 50% after 6 hours of operation in the reactor. If necessary, it may be possible to achieve higher concentrations of H₂O₂ by using additional reactors in series.

Conclusion

Electrochemical methods were used to immobilise GOx on the surfaces of electrodes. The model redox enzyme, glucose oxidase was immobilised on glassy carbon electrodes using polypyrrole, silica film, and diazonium salts to encapsulate or attach the enzyme. The highest activity and stability in terms of the rate of production of H₂O₂ was achieved with polypyrrole. This immobilisation method was subsequently used to electrochemically immobilise GOx on large surface area graphite rods to produce H₂O₂ at a rate of 602 ± 57 μMh⁻¹ with full retention of activity over a period of 7 h of continuous operation. The rods were incorporated into a flow reactor that produced H₂O₂ at a rate of 41.6 ± 0.8 μMh⁻¹ in a stable and continuous manner. Subsequent downstream use of the generated H₂O₂ can be utilised in a range of oxidation reactions. The enzymatic method described here operates under mild conditions and can be directly coupled with other enzymes that utilise H₂O₂ as a substrate. The novelty of the approach described lies in the use

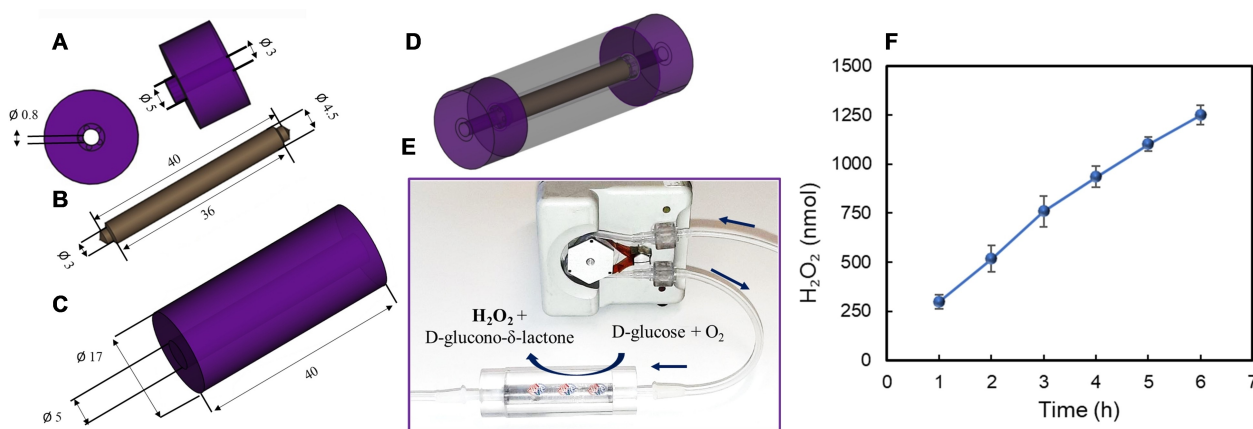


Figure 5. Computer aided design (CAD) drawing of the flow cell consisting of (A) two cap, (B) a graphite rod and (C) a cylinder (unit mm). The drawing of (D) the assembled reactor. Photograph of (E) the flow reactor system (F) The time course of the production of H₂O₂ at a PPy-GOx-NF/GRE in the flow reactor for 6 h in 0.1 M pH 7 phosphate buffer, 5 ml of 30 mM glucose, purged with O₂.

of electrochemical methods to control the location of immobilisation and to use this approach to incorporate the immobilised enzyme at the desired location in the flow reactor in a stable and active manner. Selective patterning of the enzyme occurs at defined locations as immobilisation can only occur at the surface of the electrode, not at any other point in the system. While the loading of the enzyme is high, $1.28 \times 10^{-9} \text{ mol cm}^{-2}$, it is likely that only enzyme at or close to the solution interface is catalytically active. The graphite rod can be removed easily from the system, without any requirement for centrifugation or other separation procedures. Further improvement of the system can be achieved by increasing the specific surface area of the electrode and increasing the supply of oxygen. The approach described has significant potential as a platform for the development of flow reactors that rely on the use of H_2O_2 as an oxidant. A range of enzymatic oxidation reactions are currently under examination and will be described in future reports.

Experimental Section

Reagents and materials

Hydrochloric acid (HCl, 37%), tetraethoxysilane (TEOS, 99.9%), 6-amino-2-naphthoic acid (NA), N-cyclohexyl-N'-(2-morpholinoethyl) carbodiimide metho-p-toluenesulfonate (CMC), nitrophenyl diazonium tetrafluoroborate, tetrabutylammonium tetrafluoroborate (TBATFB), acetonitrile (can), sodium nitrite, pyrrole (Py, 99% purity), Nafion® (5 wt%), dibasic and monobasic sodium phosphate, ethanol, potassium chloride, d-(+)-glucose, glucose oxidase (GOx) from *Aspergillus niger* (50000 U mg^{-1}), peroxidase from horseradish (HRP), 2,2'-azino-bis(3-ethylbenzothiazoline-6-sulfonic acid) diammonium salt (ABTS) and 4-morpholineethanesulfonic acid (MES), were obtained from Sigma-Aldrich, Ireland, Ltd. All solutions were prepared with deionised water (resistivity of $18.2 \text{ M}\Omega \text{ cm}$) from an Elgastat maxima-HPLC (Elga Purelab Ultra, UK).

Electrochemical experiments were performed with a CHI630 A potentiostat (CH Instruments, Austin, Texas). A conventional three-electrode cell using a glassy carbon (GCE, 0.07 cm^2) (CH Instruments), screen printed carbon (SPE, 0.12 cm^2) (Metrohm) or fine extruded graphite rod (GRE, 4.77 mm OD, 5.76 cm^2) (Graphite Store) as the working electrode, together with Pt wire or stainless-steel mesh as the counter electrode and an Ag/AgCl (4 M KCl) reference electrode. Prior to electrode modification, GCEs were polished with 1 micron aluminium oxide and 0.5 micron diamond lapping discs (Mason Technology Ltd.) and then sonicated in a solution of water-ethanol (1:1) for 3 minutes. GREs were polished with sandpaper (P2000) and 1 micron aluminium oxide lapping discs, cleaned by sonication in a solution of water-ethanol-acetone (1:1:1) for 9 minutes and dried in the oven. Absorbance measurements were recorded on a Cary 60 UV-Vis spectrophotometer (Agilent, USA). Glucose solutions were mixed at 25°C for 12 hours before use.

Surface modification and immobilisation of GOx

i) **GOx/aminophenyl/GCE.** GCE electrodes were immersed in acetonitrile solution (ACN), containing 1 mM nitrophenyl diazonium tetrafluoroborate and 0.1 M TBATFB. Two potential cycles over the range 0.4 to -0.3 V at a scan rate of 100 mVs^{-1} were used to graft a layer onto the electrode. The modified electro-

des were then immersed in a solution of water and ethanol (9:1 v/v) containing 0.1 M KCl. Scanning the potential between 0.7 and -1.2 V at 200 mVs^{-1} for five potential cycles was used to reduce nitrophenyl to aminophenyl groups. For electrochemical immobilisation of GOx, the modified electrodes were immersed in a solution of GOx (5 mg mL^{-1}) in phosphate buffer (0.1 M pH 7), and the potential scanned between -1.0 to 1.2 V at 200 mVs^{-1} for 25 potential cycles. Prior to utilisation, electrodes were placed in a solution of phosphate buffer (0.1 M pH 7) for 12 hours in the fridge. The surface coverage of the aminophenyl layer, normalized to the geometric area, was estimated from $\Gamma = Q/nFA$, where A is the surface area of the electrode, F the Faraday constant ($96,485 \text{ C mol}^{-1}$), n the number of electrons and Q is the charge.

ii) **GOx/naphthoic acid/GCE.** GCE electrodes were immersed in the mixture of 2 mL 6-amino-2-naphthoic acid (20 mM) prepared in acetonitrile and 2 mL NaNO_2 (5 mM) prepared in HCl (1 M), both were prepared in an ice bath. One potential cycle over the range 0.6 to -0.5 V at a scan rate of 200 mVs^{-1} was used to graft a layer onto the electrode. Then a 20 μL aliquot of a solution of GOx (9 mg mL^{-1} , in MES buffer (pH 6, 10 mM)) was drop cast onto the electrode surface and the electrodes were kept at 4°C for 1 h. Then the modified electrode was immersed in a solution of CMC (5 mM) at 4°C for 4 h. The electrodes were washed with distilled water, and the electrodes were allowed to dry at 4°C overnight.

iii) **PPy-GOx/GCE, PPy-GOx-NF/SPE and PPy-GOx-NF/GRE.** Pyrrole was distilled before use. PPy-GOx-NF/SPE and PPy-GOx-NF/GRE were prepared in a solution of Py (0.2 M) and different concentrations of Nafion® (2, 5, 10 and $20 \mu\text{L mL}^{-1}$) and GOx (1, 2, 3 and 5 mg mL^{-1}) in phosphate buffer (0.1 M pH 6). PPy-GOx/GCE was prepared in solution of Py (0.2 M) and different concentrations of GOx (1, 1.2, 2 and 5 mg mL^{-1}) in phosphate buffer (0.1 M pH 7). All solutions were stirred at 60 rpm for 90 min at 20°C . PPy-GOx/GCE was prepared using a constant potential of 0.85 V (vs. Ag/AgCl) at different electrodeposition times, while a potential of 0.7 V (vs. Ag/AgCl) was used for the preparation of PPy-GOx-NF/SPE. The electrodes were stored in air at 4°C overnight before use. PPy-GOx-NF/SPE and PPy-GOx-NF/GRE were stored in humid air at 4°C . The thickness of the PPy layer was estimated from $d = QM/nFA\rho$, where M is the molar mass of the repetitive unit (67.09 g mol^{-1}),^[60] Q the electrical charge, F the Faraday constant ($96,485 \text{ C mol}^{-1}$), A the electrode area (0.0706 cm^2), ρ the density of the polymer (1.5 g cm^{-3}),^[61,62] and n the number of electrons associated with the formation of PPy (2.25).^[60] The mechanical stability of PPy-GOx-NF/GRE was tested using adhesive tape. The modified electrodes were allowed to dry, then a small piece of adhesive tape was attached to the modified electrode surface and removed after 10 seconds.

iv) **Si-GOx/GCE.** A silica sol was typically prepared by dissolving 2.125 g TEOS, 2 mL of deionized water, and 2.5 mL of HCl (0.01 M) and subsequently mixed for 24 h using a magnetic stirrer (solution A). Solution A was diluted (1:4) with water for further use (solution B). A 100 μL aliquot of GOx (10 mg mL^{-1}) was added to 900 μL of solution B and electrodeposition performed at an applied potential of -1.2 V vs. Ag/AgCl. Electrodes were dried for 1 hour at room temperature and then stored in a refrigerator for 12 hours before use. Production and detection of H_2O_2 . The prepared electrodes were immersed in a solution of phosphate buffer (pH 7, 0.1 M) for 1 hour, followed by immersion into an unstirred solution of glucose (30 mM) prepared in phosphate buffer (pH 7, 0.1 M). The solution was saturated with oxygen and kept in the dark, GOx/naphthoic acid/GCE was immersed in a 1 ml stirred solution of glucose (60 rpm). The modified electrodes were removed from the

solutions of glucose after one hour and immersed in fresh solutions of glucose. The concentration of H₂O₂ was determined using a HRP assay with ABTS (SI).

Flow reactor design

A flow reactor was designed to incorporate the graphite rods. The reactor was prepared using an inexpensive acrylate-based material that is transparent and allows visual monitoring of the reaction and detection of air bubbles that may form inside the channel. A schematic of the reactor is designed by FreeCAD, parametric 3D modeler (Figure 5). The reactor consists of two caps and a cylinder (inner radius: 5 mm) (Figure 5A, C). The graphite rod (Figure 5B) had an accessible surface 5.08 cm² area in the reactor. The caps at both ends of the cylinder position the rods in the middle of the channel, while small grooves in the cap (Figure 5A) allow the solution to pass through the channel. An Instech P720 peristaltic pump was used to pump the solution through the channel (Figure 5E). Glucose solutions were purged with oxygen during the operation of the reactor and pumped into the channel at a flow rate of 0.02 ml min⁻¹.

Acknowledgements

This research was funded by the Science Foundation Ireland (SFI) Research Centre for Pharmaceuticals under Grant Number 12/RC/2275. X.X. acknowledges a Villum Experiment (grant No. 35844). Open Access funding provided by IReL.

Conflict of Interest

The authors declare no conflict of interest.

Data Availability Statement

The data that support the findings of this study are available from the corresponding author upon reasonable request.

Keywords: Glucose oxidase · Flow reactor · H₂O₂ generation · Electrodeposition · Polypyrrole

[1] U. Hanefeld, L. Gardossi, E. Magner, *Chem. Soc. Rev.* **2009**, *38*, 453–468.
[2] E. W. Nery, L. T. Kubota, *J. Pharm. Biomed. Anal.* **2016**, *117*, 551–559.
[3] R. A. Sheldon, S. van Pelt, *Chem. Soc. Rev.* **2013**, *42*, 6223–6235.
[4] X. Xiao, T. Siepenkoetter, P. O. Conghaile, D. N. Leech, E. Magner, *ACS Appl. Mater. Interfaces.* **2018**, *10*, 7107–7116.
[5] T. A. Hakala, F. Bialas, Z. Toprakcioglu, B. Bräuer, K. N. Baumann, A. Levin, G. A. J. Bernardes, C. F. Becker, T. P. Knowles, *ACS Appl. Mater. Interfaces.* **2020**, *12*, 32951–32960.
[6] N. Nuchtavorn, J. Leanpolchareanchai, L. Suntornsuk, M. Macka, *Anal. Chim. Acta.* **2020**, *1098*, 86–93.
[7] D. Hetemi, V. Noël, J. Pinson, *Biosensors* **2020**, *10*, 4.
[8] L. Cao, *Carrier-bound immobilised enzymes: principles, application and design*, John Wiley & Sons, **2006**.
[9] R. A. Sheldon, R. Schoevaart, L. M. V. Langen, in *Immobilisation of enzymes and cells*, Springer, **2006**, pp. 31–45.
[10] T. Jesionowski, J. Zdarta, B. Krajewska, *Adsorption* **2014**, *20*, 801–821.

[11] X. Xiao, T. Siepenkoetter, R. Whelan, U. Salaj-Kosla, E. Magner, *J. Electroanal. Chem.* **2018**, *812*, 180–185.
[12] Y. Gu, J. Wang, M. Pan, S. Li, G. Fang, S. Wang, *Sens. Actuators B* **2019**, *283*, 571–578.
[13] R. D. Milton, S. D. Minteer, *J. Electrochem. Soc.* **2014**, *161*, H3011.
[14] A. Walcarius, E. Sibottier, M. Etienne, J. Ghanbaja, *Nat. Mater.* **2007**, *6*, 602–608.
[15] O. Nadzhafova, M. Etienne, A. Walcarius, *Electrochem. Commun.* **2007**, *9*, 1189–1195.
[16] M. Rafiee, B. Karimi, S. Arshi, H. Vali, *Dalton Trans.* **2014**, *43*, 4901–4908.
[17] W. Schuhmann, C. Kranz, J. Huber, H. Wohlschläger, *Synth. Met.* **1993**, *61*, 31–35.
[18] W. Schuhmann, *Microchim. Acta* **1995**, *121*, 1–29.
[19] O. Gursoy, S. Sen Gursoy, S. Cogal, G. Celik Cogal, *Polym. Eng. Sci.* **2018**, *58*, 839–848.
[20] P. Bartlett, R. Whitaker, *J. Electroanal. Chem. Interfacial Electrochem.* **1987**, *224*, 37–48.
[21] W. Schuhmann, R. Lammert, B. Uhe, H.-L. Schmidt, *Sens. Actuators B* **1990**, *1*, 537–541.
[22] M. Hämmerle, W. Schuhmann, H.-L. Schmidt, *Sens. Actuators B* **1992**, *6*, 106–112.
[23] S. Sadki, P. Schottland, N. Brodie, G. Sabouraud, *Chem. Soc. Rev.* **2000**, *29*, 283–293.
[24] M. Singh, P. K. Kathuroju, N. Jampana, *Sens. Actuators B* **2009**, *143*, 430–443.
[25] I. Kucherenko, O. Soldatkin, D. Y. Kucherenko, O. Soldatkina, S. Dzyadevych, *Nanoscale Adv.* **2019**, *1*, 4560–4577.
[26] M. Nemiwal, T. C. Zhang, D. Kumar, *Enzyme Microb. Technol.* **2022**, *156*, 110006.
[27] X. Xiao, H.-q. Xia, R. Wu, L. Bai, L. Yan, E. Magner, S. Cosnier, E. Lojou, Z. Zhu, A. Liu, *Chem. Rev.* **2019**, *119*, 9509–9558.
[28] A. Serletti, X. Xiao, K. Shortall, E. Magner, *ChemElectroChem* **2021**, *8*, 3911–3916.
[29] B. Burek, S. Bormann, F. Hollmann, J. Bloh, D. Holtmann, *Green Chem.* **2019**, *21*, 3232–3249.
[30] K. Hernandez, A. Berenguer-Murcia, R. C. Rodrigues, R. Fernandez-Lafuente, *Curr. Org. Chem.* **2012**, *16*, 2652–2672.
[31] D. S. Choi, Y. Ni, E. Fernández-Fueyo, M. Lee, F. Hollmann, C. B. Park, *ACS Catal.* **2017**, *7*, 1563–1567.
[32] B. Yuan, D. Mahor, Q. Fei, R. Wever, M. Alcalde, W. Zhang, F. Hollmann, *ACS Catal.* **2020**, *10*, 8277–8284.
[33] D. S. Choi, H. Lee, F. Tieves, Y. W. Lee, E. J. Son, W. Zhang, B. Shin, F. Hollmann, C. B. Park, *ACS Catal.* **2019**, *9*, 10562–10566.
[34] F. Tieves, S. J. P. Willot, M. M. C. H. van Schie, M. C. R. Rauch, S. H. H. Younes, W. Zhang, J. Dong, P. Gomez de Santos, J. M. Robbins, B. Bommarius, *Angew. Chem. Int. Ed.* **2019**, *58*, 7873–7877; *Angew. Chem.* **2019**, *131*, 7955–7959.
[35] S. C. Perry, D. Pangotra, L. Vieira, L.-I. Csepei, V. Sieber, L. Wang, C. P. de León, F. C. Walsh, *Nat. Chem. Rev.* **2019**, *3*, 442–458.
[36] J. Zhou, X. An, H. Lan, H. Liu, J. Qu, *Appl. Surf. Sci.* **2020**, *509*, 144875.
[37] H. Qiu, Y. Li, G. Ji, G. Zhou, X. Huang, Y. Qu, P. Gao, *Bioresour. Technol.* **2009**, *100*, 3837–3842.
[38] L. Chen, A. Y. Lyubimov, L. Brammer, A. Vrielink, N. S. Sampson, *Biochemistry* **2008**, *47*, 5368–5377.
[39] Y. Ni, E. Fernández-Fueyo, A. G. Baraibar, R. Ullrich, M. Hofrichter, H. Yanase, M. Alcalde, W. J. van Berkel, F. Hollmann, *Angew. Chem. Int. Ed.* **2016**, *55*, 798–801; *Angew. Chem.* **2016**, *128*, 809–812.
[40] S. B. Bankar, M. V. Bule, R. S. Singhal, L. Ananthanarayan, *Biotechnol. Adv.* **2009**, *27*, 489–501.
[41] P. C. Pereira, I. W. Arends, R. A. Sheldon, *Process Biochem.* **2015**, *50*, 746–751.
[42] D. Jung, C. Streb, M. Hartmann, *Microporous Mesoporous Mater.* **2008**, *113*, 523–529.
[43] A. Zaks, A. V. Yabannavar, D. R. Dodds, C. A. Evans, P. R. Das, R. Malchow, *J. Org. Chem.* **1996**, *61*, 8692–8695.
[44] A. Zaks, D. R. Dodds, *JACS* **1995**, *117*, 10419–10424.
[45] F. van de Velde, N. D. Lourenço, M. Bakker, F. van Rantwijk, R. A. Sheldon, *Biotechnol. Bioeng.* **2000**, *69*, 286–291.
[46] J. Rocha-Martin, S. Velasco-Lozano, J. M. Guisán, F. López-Gallego, *Green Chem.* **2014**, *16*, 303–311.
[47] I. Kocak, M. A. Ghanem, A. Al-Mayouf, M. Alhoshan, P. N. Bartlett, *J. Electroanal. Chem.* **2013**, *706*, 25–32.
[48] T. Siepenkoetter, U. Salaj-Kosla, X. Xiao, P. Ó. Conghaile, M. Pita, R. Ludwig, E. Magner, *ChemPlusChem* **2017**, *82*, 553–560.
[49] P. A. Brooksby, A. J. Downard, *Langmuir* **2004**, *20*, 5038–5045.

- [50] H. Du Toit, M. Di Lorenzo, *Electrochim. Acta* **2014**, *138*, 86–92.
- [51] I. Mazurenko, M. Etienne, O. Tananaiko, V. Zaitsev, A. Walcarius, *Electrochim. Acta* **2012**, *83*, 359–366.
- [52] F. Qu, R. Nasraoui, M. Etienne, Y. B. Saint Côme, A. Kuhn, J. Lenz, J. Gajdzik, R. Hempelmann, A. Walcarius, *Electrochem. Commun.* **2011**, *13*, 138–142.
- [53] H. Kanso, M. Begoña González García, S. Ma, R. Ludwig, P. Fanjul Bolado, D. Hernández Santos, *Electroanalysis* **2017**, *29*, 87–92.
- [54] J.-C. Vidal, E. Garcia, J.-R. Castillo, *Biosens. Bioelectron.* **1998**, *13*, 371–382.
- [55] Y. Li, R. Qian, *Electrochim. Acta* **2000**, *45*, 1727–1731.
- [56] B. K. Shrestha, R. Ahmad, H. M. Mousa, I.-G. Kim, J. I. Kim, M. P. Neupane, C. H. Park, C. S. Kim, *J. Colloid Interface Sci.* **2016**, *482*, 39–47.
- [57] M. ElKaoutit, I. Naranjo-Rodríguez, M. Domínguez, J. L. Hidalgo-Hidalgo-de-Cisneros, *Appl. Surf. Sci.* **2011**, *257*, 10926–10935.
- [58] Y. M. Uang, T. C. Chou, *Electroanalysis* **2002**, *14*, 1564–1570.
- [59] X. Xiao, H. Li, P. Si, *Talanta* **2013**, *116*, 1054–1059.
- [60] T. Patois, B. Lakard, S. Monney, X. Roizard, P. Fievet, *Synth. Met.* **2011**, *161*, 2498–2505.
- [61] M. Salmon, A. Diaz, A. Logan, M. Krounbi, J. Bargon, *Mol. Cryst. Liq. Cryst.* **1982**, *83*, 265–276.
- [62] S. Holdcroft, B. L. Funt, *J. Electroanal. Chem. Interfacial Electrochem.* **1988**, *240*, 89–103.

Manuscript received: March 22, 2022

Revised manuscript received: June 24, 2022

Accepted manuscript online: July 4, 2022